Article

Not peer-reviewed version

Fabrication of Sodium Alginate/Polyethyleneimine/ Polyvinyl Alcohol Multilayer Composite Electrospun Nanofiber Membrane for Cu2+ Removal

Boshi Xie , Ziao Zhang , Yujie Lu , Lijuan Cui , Chao Xu , Weijian Shi , Shuping Wu *

Posted Date: 23 April 2024

doi: 10.20944/preprints202404.1548.v1

Keywords: Electrospinning; nanofiber membranes; multilayer composite; sodium alginate; polyethyleneimine; copper ion removal

 doi:10.20944/preprints202404.1548.v1

Article

Fabrication of Sodium Alginate/Polyethyleneimine/ Polyvinyl Alcohol Multilayer Composite Electrospun Nanofiber Membrane for Cu^{2+} Removal

Boshi Xie, Ziao Zhang, Yujie Lu, Lijuan Cui, Chao Xu, Weijian Shi and Shuping Wu *

Institute of Polymer Materials, School of Materials Science & Engineering, Jiangsu University, Zhenjiang, Jiangsu Province, 212013, China
* Correspondence: shupingwu@ujs.edu.cn

Abstract: In this study, multilayer composite nanofiber membranes of sodium alginate (SA) /polyethyleneimine (PEI)/polyvinyl alcohol (PVA) was fabricated via electrospinning technique to enhance the adsorption of Cu^{2+} from wastewater. The preparation and adsorption mechanisms of the SA/PEI/PVA nanofiber membranes were analyzed by utilizing analytical techniques such as SEM, FTIR, EDS, UV-vis, XRD, and TG. The obtained nanofiber membrane characterized by small diameter, high uniformity, and extensive surface area, demonstrate significant potential for heavy metal ion filtration. Optimal spinning parameters were identified, including a voltage of 19.5 KV, a distance of 8 cm, and specific mass ratios (SA: PEI: PVA, 1:2:6) and injection speeds (8 μL/min) and. The resulting nanofibers with an average diameter of 112.5 nm exhibited excellent morphology and high efficiency, retaining over 85% adsorption capacity for Cu^{2+} in initial tests and maintaining above 80% efficacy through four successive filtration cycles.

Keywords: electrospinning; nanofiber membranes; multilayer composite; sodium alginate; polyethyleneimine; copper ion removal

1. Introduction

Water is essential for human survival, making the availability and quality of freshwater a critical concern. In the 21st century, the rapid advancement of modern industry and agriculture has escalated environmental pollution to a global challenge, with water pollution standing out as a particularly severe issue. This pollution stems from various sources, including indiscriminate industrial wastewater discharge, urban sewage, and uncontrolled pesticide and fertilizer use, leading to widespread contamination of water bodies. Such pollution poses a significant threat to both aquatic life and human health. Among the pollutants, heavy metals are especially concerning due to their toxicity and persistence in the environment; they are non-biodegradable and accumulate in the ecosystem, magnifying their impact through the food chain [1–3]. Even at low initial concentrations, heavy metals can eventually endanger human health. Given these challenges, there is a pressing need for effective water purification methods. Membrane separation technology, known for its low energy requirements, small footprint, and high efficiency, has become a preferred solution in water treatment efforts [4–6].

Electrospinning has emerged as a prominent method for fabricating nanofiber materials, gaining significant attention for its role in creating adsorbent membranes. This technique offers distinct advantages over traditional spinning methods, including ultra-high porosity, extensive specific surface area, and consistent fiber diameter distribution, making it highly suitable for membrane processing applications. As a versatile and efficient technology, electrospinning allows for the use of varied raw materials tailored to specific targets. Its applications extend across filtration and

 doi:10.20944/preprints202404.1548.v1

separation, composite reinforcement, tissue engineering, biocatalysis, and controlled drug release [7–11]. The theoretical foundations of electrospinning were first established in the late 19th century by Lord Rayleigh. In 1882, Lord Rayleigh investigated the behavior of liquid droplets on charged surfaces and described the conditions under which these droplets would become unstable and disintegrate, which is a fundamental aspect of electrospinning. This work laid the groundwork for understanding how electric forces can deform and disperse liquids, which is central to the process of electrospinning, where electrically charged jets of polymer solutions or melts are used to produce fibers. Further deepening their understanding, researchers established the core principles of electrostatic spinning. By applying high-voltage electrostatic forces to a polymer melt or solution, a strong electric field is created between the polymer in the capillary tube and the grounding device. This setup imparts a uniform positive charge to the polymer, forming suspended charged droplets at the capillary's end. These droplets are then drawn into a conical shape, known as the Taylor cone. When the electric field strength surpasses the surface tension, the droplets are propelled from the capillary tip, stretch towards the grounding device under the electric forces, and form nanofibers.

Electrospun nanofibers have proven to be exceptional nanomaterials with significant potential for removing heavy metal ions. Yang et al. developed amino-functionalized chitosan (CS) electrospun membranes by sequentially grafting poly(glycidyl methacrylate) (PGMA) and polyethyleneimine (PEI) onto CS fibers, with the successful incorporation of amino groups verified using XRD, ATR-FTIR, and XPS techniques [12]. The CS-PGMA-PEI membrane rapidly reached adsorption equilibrium within 60 minutes, demonstrating maximum adsorption capacities for Cr(VI), Cu(II), and Co(II) at 138.96, 69.27, and 68.31 mg/g, respectively, according to the Langmuir model. This study highlights the membrane's potential for efficient water purification, showing notable reproducibility and stability in removing heavy metal ions. In our previous research, we developed carboxymethyl cellulose (CMC)/polyvinyl alcohol (PVA) composite nanofiber membranes through electrostatic spinning, utilizing CMC and PVA with glutaraldehyde as a cross-linker, and characterized them using techniques such as SEM, FTIR, TGA, UV, and energy spectrum analysis [13]. The optimized spinning parameters (23 KV and 2 μL/min) resulted in fibers with a reduced diameter of 183 nm, indicating finer and more uniformly distributed fibers. The membranes demonstrated high chemical adsorption efficiencies for Cu^{2+} and Cr^{6+} with retention rates of 97.2% and 98.8%, respectively, and adsorption capacities were 26.34 $mg \cdot g^{-1}$ for Cu^{2+} and 28.93 $mg \cdot g^{-1}$ for Cr^{6+}, consistent with the pseudo-second-order kinetic model and the Langmuir isotherm. At the same time, our team successfully synthesized a chitosan (CS)/polyvinylpyrrolidone (PVP)/polyvinyl alcohol (PVA) hollow nanofiber membrane (CS/PVP/PVA-HNM) via coaxial electrospinning [10]. This membrane demonstrated remarkable permeability and adsorption separation. Specifically, the CS/PVP/PVA-HNM had a pure water permeability of 4367.02 $L \cdot m^{-2} \cdot h^{-1} \cdot bar^{-1}$. The hollow electrospun nanofibrous membrane exhibited a continuous interlaced nanofibrous framework structure with the extraordinary advantages of high porosity and high permeability. The rejection ratios of CS/PVP/PVA-HNM for Cu^{2+}, Ni^{2+}, Cd^{2+}, Pb^{2+}, malachite green (MG), methylene blue (MB) and crystal violet (CV) were 96.91 %, 95.29 %, 87.50 %, 85.13 %, 88.21 %, 83.91 % and 71.99 %, and the maximum adsorption capacities were 106.72, 97.46, 88.10, 87.81, 53.45, 41.43, and 30.97 $mg \cdot g^{-1}$, respectively. This work demonstrates a strategy for the synthesis of hollow nanofibers, which provides a novel concept for the design and fabrication of highly efficient adsorption and separation membranes.

Sodium alginate (SA), a natural polysaccharide extracted from various species of brown algae including macroalgae and kelp, is a linear block copolymer consisting of β-D-mannuronic acid and α-L-glucuronic acid, with the molecular formula $(C_6H_7NaO_6)_n$. It is characterized by a high density of carboxyl (-COOH) and hydroxyl (-OH) functional groups along its molecular chain[14–16]. These groups enable sodium alginate to effectively bind with divalent or higher-valency metal ions M^{n+} ($n \geq 2$), facilitating the ion-exchange processes where H^+ and Na^+ are replaced, forming a complex three-dimensional gel network enriched with M^{n+}. This property makes sodium alginate an ideal candidate for use as an investment material in a variety of applications [17–21]. Sodium alginate is non-toxic, has excellent film-forming ability, and has excellent biocompatibility and biodegradability, and is widely used in various industries. These include food production as thickeners and stabilizers;

 doi:10.20944/preprints202404.1548.v1

pharmaceuticals, for use in drug delivery systems; cosmetics, for their moisturizing properties; and the textile industry, especially in dyeing processes. Its versatility and environmental friendliness underscore its growing importance in sustainable industrial practices, reflecting a shift toward more environmentally friendly materials in technology and product development.

Polyethyleneimine (PEI), also known as polyazacyclopropane, is a water-soluble macromolecule with the highest known cationic charge density among organic polymers. PEI excels in water treatment applications due to its dense amine groups—primary, secondary, and tertiary[22–26]. These groups facilitate the binding of heavy metal ions in wastewater through mechanisms like ion-exchange, electrostatic interactions, chelation, and coordination, leading to high adsorption capacity. PEI's effectiveness is highlighted in various studies, including those by Gao et al., who immobilized soluble PEI using polydopamine (PDA) polymerization, facilitating effective Pb^{2+} removal through a cooperative adsorption mechanism that leverages charged SO_3H groups within a polystyrene matrix and in-situ PDA formation at room temperature [27]. This hybrid adsorbent demonstrated exceptional selectivity and efficiency, achieving rapid lead removal kinetics, excellent sorption-regeneration properties, and an outstanding capacity for treating Pb-contaminated water with potential applicability to other metals like Fe^{3+}, Cu^{2+}, and Ni^{2+}. For instance, Bucatariu et al. modified spherical silica microparticles with linear and branched poly(ethyleneimine) (PEI) chains through layer-by-layer deposition involving a copper complex and poly(acrylic acid), followed by selective cross-linking and removal of copper and PAA, to create functional silica/$(PEIL)_{10}$ and silica/$(PEIB)_{10}$ composites [28]. These composites demonstrated effective sorption of heavy metals like Cu^{2+}, Ni^{2+}, Co^{2+}, and Cd^{2+} in batch and column experiments under noncompetitive conditions. Additionally, Tofighy et al. developed a positively charged membrane using hyperbranched polyethyleneimine (HPEI) as a crosslinking agent through a vacuum-filtration method, aimed at efficiently removing divalent heavy metal ions from contaminated water [29]. The resulting HPEI crosslinked membrane demonstrated excellent performance, highlighted by its ability to selectively reject heavy metal ions and maintain effectiveness over multiple regeneration cycles, indicating its potential for repeated use in water purification applications.

In this study, we aimed to fabricate multilayer composite nanofibrous membranes using three polymer raw materials: SA, PEI, and PVA. SA and PEI were chosen for their effective functional groups that facilitate Cu^{2+} adsorption, while PVA served as a co-spinning solution and carrier, enhancing the filament-forming properties essential for electrospinning. The spinning process involved the preparation of two hybrid spinning solutions, SA/PVA and PEI/PVA, which were alternately and cyclically spun using electrospinning to create nanofiber membranes with sufficient thickness for filtration. The resulting nanofiber membranes, theoretically insoluble in water, exhibited significant hydrogen bonding interactions within SA and PVA as well as between PEI and PVA, and interlayer hydrogen bonding between SA and PEI, enhancing the structural integrity. These multilayer membranes were subjected to both single and repeated Cu(II) filtration tests, with their performance and structural characteristics analyzed using SEM, EDS, FTIR, UV-vis, XRD, and TG. The objective of this study was to explore the feasibility and efficiency of using electrospun multilayer composite nanofibrous membranes for the adsorption and removal of Cu(II) from aqueous solutions.

2. Experimental

2.1. Materials

Sodium alginate, polyethyleneimine, polyvinyl alcohol, sodium diethyldithiocarbamate trihydrate (copper reagent) and copper chloride dihydrate produced by Sinopharm Chemical Reagent Co.

 doi:10.20944/preprints202404.1548.v1

2.2. Solution Preparation

2.2.1. SA Solution Preparation

97.00 g of deionized water was added to a 250 mL conical flask and set aside on a magnetic stirrer. 3.00 g of sodium alginate solid powder was dissolved into deionized water. When all the sodium alginate powder has been added, seal the bottle with plastic wrap. The stirring speed was then adjusted to 500 rpm and stirring was continued for 8 h at room temperature to ensure complete dissolution of sodium alginate. Once completed, label the solution, and set aside for later use.

2.2.2. PEI Solution Preparation

In the preparation of PEI solution, a quantity of PEI was first removed using a syringe. Subsequently, a 50 ml beaker was placed on an analytical balance and the balance was adjusted to zero. Next, 3.00 g of PEI was accurately weighed and added to the beaker. Thereafter, 47.00 g of deionised water was added to the beaker to dissolve the PEI. This solution was transferred to a 250 ml conical flask, and again using the beaker in which the PEI had been dissolved, 50.00 g of deionised water was weighed and added to the conical flask. After completing all additions, the conical flask was sealed with cling film to avoid contamination. Finally, the sealed conical flask was placed in an ultrasonic cleaner and sonicated for 15 minutes at room temperature to ensure that the PEI was completely dissolved and evenly distributed. After treatment, the conical flasks were labelled and set aside.

2.2.3. PVA Solution Preparation

95.00 grams of deionized water were added to a 250 ml conical flask, which was then equipped with a magnetic stir bar for later use. Using precise measurements, 5.00 grams of PVA solid particles were weighed and added to the flask containing the deionized water. To avoid any contamination during the process, the flask's opening was securely sealed with cling film. The PVA pellets were then left to soak at room temperature for 4 h, allowing them to fully absorb the water and swell. The flask was placed on a heated stirrer, with the temperature set to 90°C and the stirring speed set to medium. Continuous heating and stirring for 6 h ensured complete dissolution of the PVA granules into a uniform solution. Once the process was completed, the flasks were labeled and set aside for further use in subsequent experiments.

2.2.4. Hybrid Electrospinning Solution Preparation

In the preparation of spinning solution, the first step was the mixing of SA and PVA. The steps were as follows: 8 g of SA solution was accurately weighed into a 50 ml centrifuge tube according to the mass ratio of SA to PVA of 1:3, and then 24 g of PVA solution was added. Mixing was carried out using a vortex mixer to ensure that the two solutions were well incorporated. Afterwards, the mixture was shaken at room temperature for 5 min to further promote homogeneous mixing. To eliminate air bubbles from the mixture, the mixture was sonicated for 10 minutes using an ultrasonic cleaner. After treatment, the tube was labelled "No. 1" and set aside.

Next, a mixture of PEI and PVA was prepared. The mixing ratio of PEI to PVA was 1:4. First, 7 g of PEI solution was accurately weighed into another 50 ml centrifuge tube, followed by 28 g of PVA solution. Mix using the same vortex mixer to ensure that the solution is well mixed. After 5 minutes of shaking at room temperature, the same was carried out for 10 minutes using an ultrasonic cleaner to remove air bubbles from the mixture. After completing these steps, the centrifuge tubes were labelled "No. 2" for subsequent use.

2.2.5. Preparation of Cu^{2+} Solutions with Copper Reagents

To prepare the Cu^{2+} solution, 1.00 g of $CuCl_2$ was first precisely weighed and dissolved in a small volume of deionised water, then transferred to a 1-liter volumetric flask. The original beaker was rinsed three times with deionised water to ensure all residues were transferred. Deionised water was

 doi:10.20944/preprints202404.1548.v1

then added to the flask up to the 1 L mark to create a base solution of 1 g/L Cu^{2+}. This solution was further diluted to obtain concentrations of 10 mg/L, 8 mg/L, 6 mg/L, 4 mg/L, and 2 mg/L, with 300 mL prepared for each concentration, all properly labelled.

Similarly, for the copper reagent, 1.00 g of sodium diethylthiocarbamate trihydrate was weighed, dissolved, and transferred into a 1 L volumetric flask. The beaker used was washed three times and the flask was filled to the 1-liter mark to produce a 1 g/L solution of the copper reagent. These meticulous steps ensured the accurate preparation of the Cu^{2+} solution and copper reagent, making them ready for further experimental use.

2.3. Preparation of SA/PEI/PVA Multilayer Composite Nanofiber Membrane

The experiment involved the electrospinning of two mixed liquids, designated as No. 1 and No. 2. Initially, the liquids were drawn into syringes and spun under controlled conditions. The process began by wrapping a circle of tin foil around the receiving drum to aid in the removal of the nanofiber membrane. A zero wire connected the voltage device to the drum, and the ground wire was accessed. After verifying the connections, the experiment commenced. Using the No. 1 syringe, the liquid was injected at a rate of 4-10μL/min using an automatic liquid supply pump. The needle-to-drum distance was maintained between 5-15cm, and the voltage was set between 17-20kV. After injecting 0.5ml, spinning was paused to switch to the No. 2 syringe. This syringe was used to inject liquid at a rate of 8-12μL/min under the same distance and voltage settings. This process was repeated, alternating between the two syringes, until a total volume of more than 10mL was spun. Once complete, the nanofiber film was carefully removed from the tin foil, sealed in a bag, labeled, and stored in a desiccator for future use. The resultant nanofibrous membranes, characterized by their multilayer structure and appropriate thickness, are suitable for filtering heavy metal ions and various assay characterizations.

2.4. Cu^{2+} Filtration

The setup of the filtration apparatus begins with assembling the necessary components: a top cover, a funnel filter cup, a sand core filter head, and an Erlenmeyer flask. These are arranged vertically from top to bottom and held securely in place by stainless steel clamps to maintain stability throughout the process. The lower section of the sand core funnel is attached to a conduit that directs the filtrate straight into the Erlenmeyer flask.

To prepare the filter membrane, a nanofiber membrane is first sized by tracing and cutting out a circle that matches the diameter of the sand core funnel using a compass and scissors. This membrane is then sandwiched between two filter papers of the same size to prevent any damage from the filtration hardware. This assembly is then placed on the sand core funnel. The setup is completed by connecting a through-hole beaker to the sand core funnel with a sealing film and a clamp to ensure a tight, leak-free connection.

Before initiating the filtration, 100 mL of a pre-prepared 8 mg/L Cu^{2+} solution is added to the through-hole beaker. After securing the top cap, the system is left to allow the solution to gradually pass through the nanofiber membrane into the Erlenmeyer flask below. Once filtration is complete, the filtrate is collected and prepared for UV analysis. For assessing the membrane's reusability and durability, several filtration cycles are performed. Each cycle uses 80 mL of the 8 mg/L Cu^{2+} solution, and after each use, the nanofiber membrane is carefully sealed and stored. The cycles are conducted every 8 h, totaling six repetitions. The filtrate from each cycle is gathered and marked for subsequent evaluation and testing. This procedure not only evaluates the membrane's filtration capabilities but also tests its stability and reliability for repeated use.

2.5. Membrane Characterization

The morphology of the multilayer composite nanofiber membranes was observed using a field emission scanning electron microscope (NovaNano450, FEI, USA). The membrane surface was analyzed for elements using an X-ray spectrometer (Octane Plus, EDAX, USA). The nanofiber

 doi:10.20944/preprints202404.1548.v1

membranes, SA solid powder and PVA solid powder were characterized on an X-ray diffraction analyzer with a scanning range of 10-80° (2θ). The prepared SA/PEI/PVA multilayer composite nanofiber membranes were placed in a standard thermogravimetric analyzer (STA449F3, NETZSCH, Germany) with an atmosphere of air, a ramp rate of 10 K/min, and a test temperature range of 20-300°C. The nanofiber membranes were then analyzed in a standard thermogravimetric analyzer (STA449F3, NETZSCH, Germany). The prepared SA/PEI/PVA multilayer composite nanofiber membrane samples were oven-dried, ground and pressed with potassium bromide, and then scanned and analyzed in the infrared with a Fourier Transform infrared absorption spectrometer (FTIR, Nicolet iS10, Thermo Fisher Scientific, USA) in the wavelength range of 4000-500cm^{-1}. The 10 mg/L, 8 mg/L, 6 mg/L, 4 mg/L, and 2 mg/L Cu^{2+} solutions configured were detected with a UV-visible spectrophotometer, and the absorbance-concentration relationship was analyzed by the five-point fitting method. Six cuvettes were prepared and 3 ml of 10mg/L, 8mg/L, 6mg/L, 4mg/L, 2mg/LCu^{2+} solution was measured in a cylinder and added into five quartz cuvettes, and the sixth quartz cuvette was filled with 3 ml of deionized water to serve as the baseline and control. Two drops of copper reagent configured were added to the quartz cuvettes with Cu^{2+} solution, and scanned and analyzed by UV-visible spectrophotometer to plot absorbance versus concentration for the next step of filtration detection. The assay method for the filtrate to be tested is the same as above, which is to take 3 ml of filtrate and add two drops of copper reagent. The detection method for recirculation filtration is the same as above.

3. Results and Discussion

3.1. SEM Analysis of SA/PEI/PVA Multilayer Composite Nanofiber Membrane

To observe the microstructure of SA/PEI/PVA multilayer composite nanofibrous membranes, we carried out SEM analysis, of which representative ones were selected for analysis, and fiber diameter analysis was carried out for the ones with better morphology, as shown in Figure 1. Through repeated experiments and adjusting different spinning process parameters, we obtained a more complete set of spinning parameters. As shown in Figure 1, the adopted SA: PEI: PVA ratios were 3:5:9 and 1:2:6, respectively. Comparison of the results in Figures 1A and 1B showed that the fibre morphology obtained from spinning was more obvious and of higher quality under these parameters. By decreasing the jetting speed of the spinning solution, the blobs on the nanofibres can be significantly reduced. In addition, by slightly increasing the spinning voltage, as shown in Figure 7C, we observed a significant improvement in the spinning effect, with enhanced filamentation of the spun nanofibre film and no more blobs on the fibre surface. These adjustments optimised the spinning process and improved the quality of the nanofibrous membranes.

The fibre diameter measurements were analysed in Figure 2C, and the results are shown in Figure 2D. The analysis results show that the fibre diameter of SA/PEI/PVA multilayer composite nanofiber membrane spun with the data of Figure 2C is concentrated between 70 nm-160 nm, and the average diameter reaches 112.5 nm. The fibre diameter of the spun multilayer composite nanofiber membrane is more uniform, and the fibre diameter can reach the expected effect.

By controlling the distance, spinning liquid mixing ratio, temperature and humidity unchanged, and adjusting the voltage and jetting speed, it was obtained that a slight increase in the voltage, as well as a decrease in the jetting speed in this system, for the spinning process, the appearance of small spheres on the nanofibers, as well as nanofiber homogeneity has been changed in a more favourable way.

 doi:10.20944/preprints202404.1548.v1

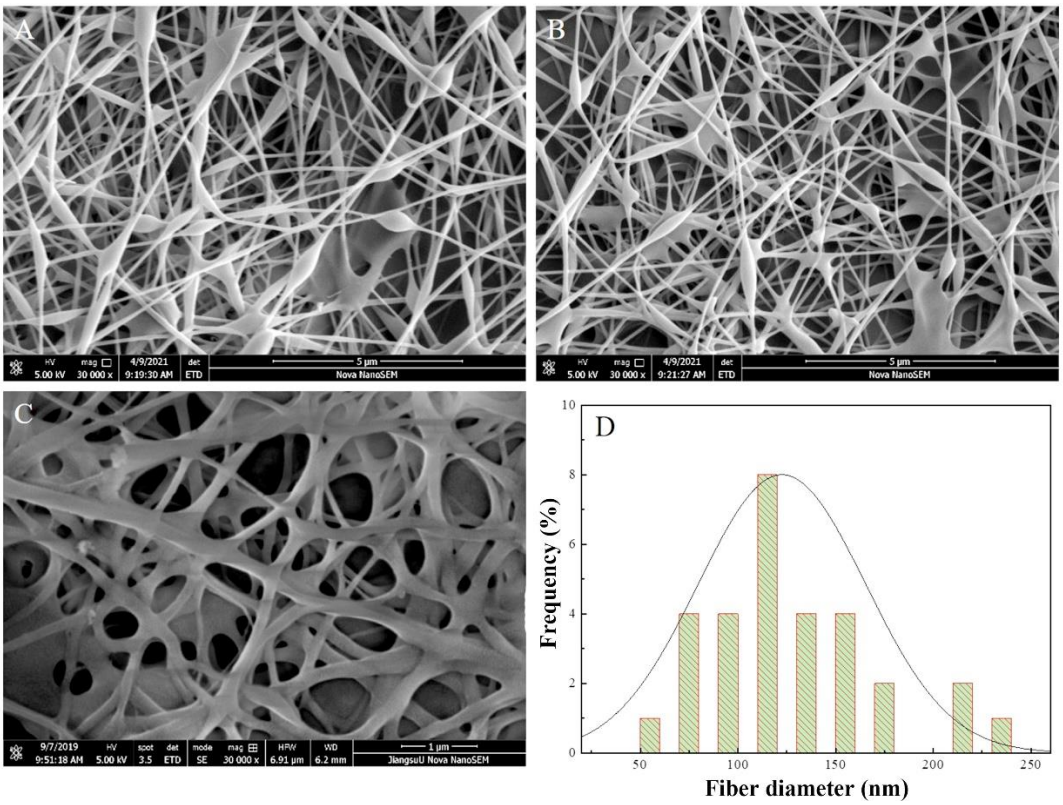

Figure 1. SEM images of the multilayer composite nanofiber membranes with different mass ratio of SA: PEI: PVA. (A) 3:5:9, 19 kV, 8cm; (B) 1:2:6, 19 kV, 8cm; (C) 1:2:6, 19.5 kV, 8cm. (D) Composite nanofiber membrane fiber diameter distribution histograms.

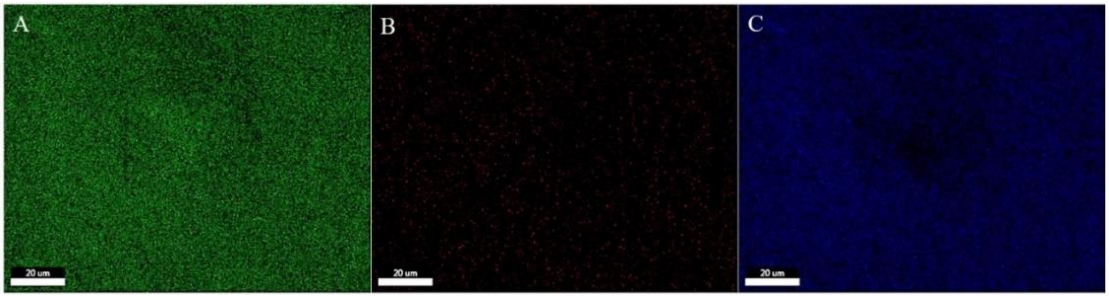

Figure 2. Elemental map of SA/PEI/PVA multilayer composite nanofiber membranes before filtration. (A), C; (B), N; (C) O.

3.2. EDS Analysis of SA/PEI/PVA Multilayer Composite Nanofiber Membranes

To assess the adsorption of heavy metal ions by SA/PEI/PVA multilayer composite nanofibrous membranes before and after filtration, we conducted Energy Dispersive X-ray Spectroscopy (EDS) scans on the membranes used before and after filtration, and recorded the elemental content. The originated membranes and those preserved after filtration with their elemental distributions shown in Figures 2 and 3, and the elemental data listed in Tables 2 and 3, respectively. In Figure 2, green markers indicate carbon elements (A), red markers indicate nitrogen elements (B), and blue markers indicate oxygen elements (C). The EDS results indicate that the surface elements of the SA/PEI/PVA multilayer composite nanofibrous membranes are consistent with the elements found in the raw materials SA, PEI, and PVA, with no other impurities detected. Fig.3 presents the EDS scan results of the membranes after filtration, where green, red, and blue markers represent carbon, nitrogen, and oxygen elements, respectively, like Figure 2. The yellow markers (D) indicate the presence of copper elements, showing that the post-filtration nanofibrous membranes retained the elements from the

 doi:10.20944/preprints202404.1548.v1

raw materials and successfully adsorbed Cu^{2+} from the solution. The uniform distribution of copper elements (as shown in Figure 3D) confirms the uniform distribution of Cu^{2+} adsorbing functional groups on the membrane, further validating its effectiveness in adsorbing heavy metal ions.

Table 1. SA/PEI/PVA multilayer composite nanofiber membrane filtration pre-pointing EDS element percentage table.

Wt.%		
C	N	O
63	1	35

Table 2. SA/PEI/PVA multilayer composite nanofiber membrane filtration after punching EDS element percentage table.

Wt.%			
C	N	O	Cu
75	1	23	1

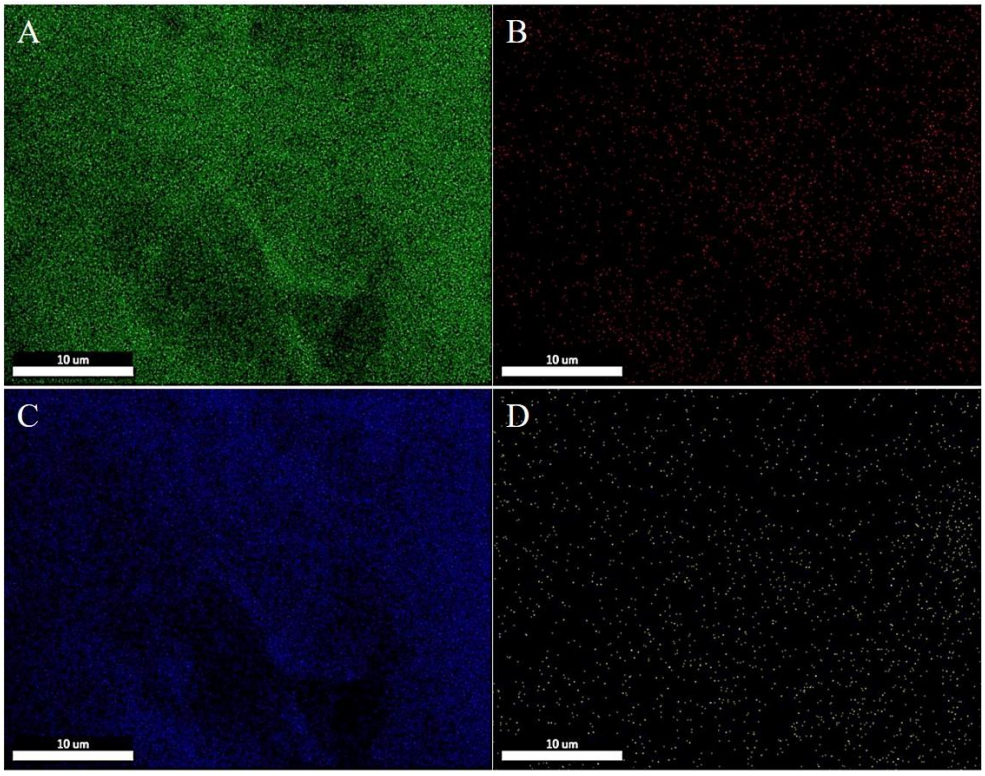

Figure 3. EDS elemental maps of SA/PEI/PVA multilayer composite nanofiber membrane filtration after filtration. (A) C; (B) N; (C) O; (D) Cu.

3.3. XRD Analysis of SA/PEI/PVA Multilayer Composite Nanofiber Membrane

The crystalline properties of SA/PEI/PVA multilayer composite nanofiber membranes were investigated using XRD. The results of this analysis are displayed in Figure 4, which features the XRD test and analysis images for the SA/PEI/PVA multilayer composite nanofiber membranes. The analysis reveals that pure SA has limited crystallization capability, while pure PVA exhibits excellent crystallization properties. The multilayer composite nanofiber membrane, created by incorporating SA and PEI, integrates the characteristics of all three materials. It retains the crystalline properties of PVA and displays the amorphous peak of SA at 19.8°, indicating a uniform blend of the three components within the multilayer composite nanofiber membrane.

 doi:10.20944/preprints202404.1548.v1

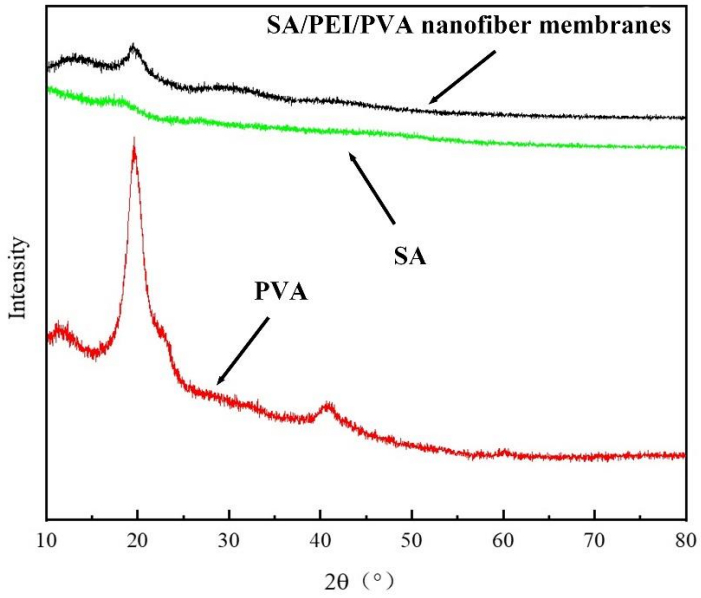

Figure 4. XRD of SA/PEI/PVA multilayer composite nanofiber membrane.

3.4. FTIR Analysis of SA/PEI/PVA Multilayer Composite Nanofiber Membrane

To analyse and verify the effective functional groups of Cu^{2+} adsorbed on SA/PEI/PVA multilayer composite nanofiber membranes, we performed FTIR analysis and the results are shown in Figure 5. The absorption peaks at 1106.5cm^{-1} and 1384.7 cm^{-1} represent the stretching and bending vibration of the carboxyl group (-COOH). Compared with the pre-filtration, the absorption peaks at 1106.5 cm^{-1} and 1384.7 cm^{-1} have obviously disappeared from the membrane after filtration, which also verifies that the sodium alginate embedding mechanism described in the previous section is used to adsorb and remove the Cu from the solution. The absorption peaks at 1647 cm^{-1} represent iminos ($-NH_2$) and C-H in alkanes, and the absorption peaks on the membrane after filtration are much reduced compared with those before filtration, which proves that the iminos are also consumed during the filtration of Cu^{2+}, which is related to the filtration of Cu^{2+}.

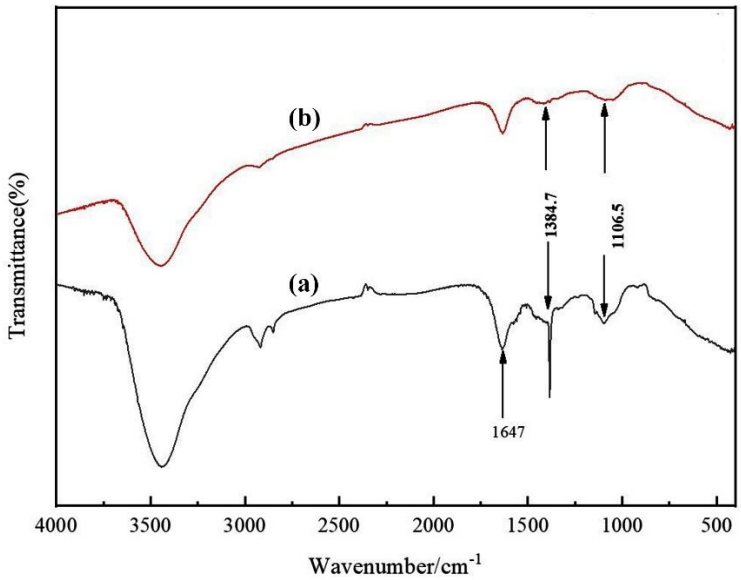

Figure 5. FTIR of nanofiber membrane before (a) and after (b) filtration.

 doi:10.20944/preprints202404.1548.v1

3.5. TG Analysis of SA/PEI/PVA Multilayer Composite Nanofiber Membranes

In addition to the research basis of microstructure, the prepared SA/PEI/PVA multilayer composite nanofiber membranes were evaluated in terms of structural properties. TG analysis was conducted on these nanofibers, with the results displayed in Figure 6. The detection temperature of TG was increased from room temperature to 300the atmosphere was air, and the rate of temperature increase was selected to be 10 K/min, and the conditions of the detection were closer to those of our filtration. The filtration of copper ions was carried out at room temperature, and according to the results of TG, the mass change of the spun nanofiber membrane was -4.49% at 100°C. At room temperature, our spun multilayer composite nanofiber membrane is more stable and is not easily affected by the ambient temperature during the filtration process.

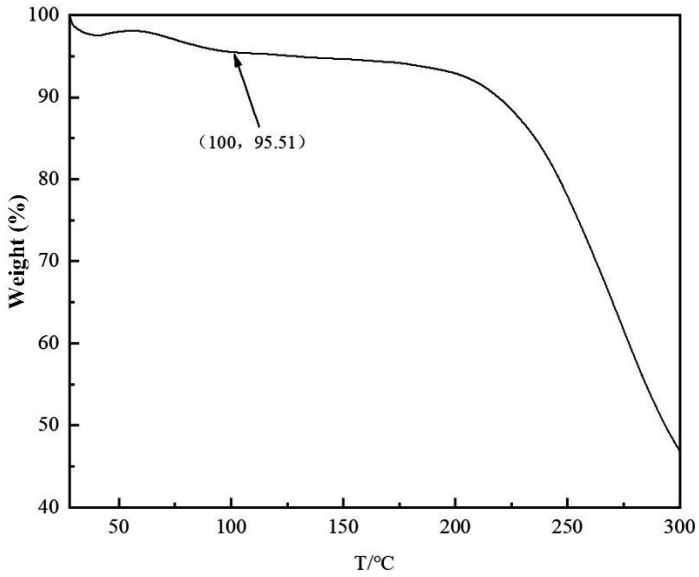

Figure 6. TG of SA/PEI/PVA multilayer composite nanofiber membrane.

3.6. Filtration Efficiency of Cu^{2+} via UV-vis

To assess the filtration efficiency of SA/PEI/PVA multilayer composite nanofibers for Cu^{2+} ions, the filtrate was calculated and analysed using UV-vis spectroscopy. This method measures the absorption of visible light by different concentrations of Cu^{2+}, where each solution correlates to a specific absorbance value. Since Cu^{2+} ions themselves do not absorb light, a copper reagent was added to enable light absorption. To maintain consistency across all test samples, an equal concentration and volume of copper reagent were added to each sample, ensuring uniformity in the quantity of reagent filtered. The results were presented in Figure 7, which illustrated the UV-vis spectroscopic analysis of the samples. Figure 7A displays the detection results for the standard concentration of Cu^{2+}, where the absorption peak of Cu^{2+} appears around 450 nm. By analyzing the absorbance of Cu^{2+} in five different standard concentration gradients, we created the concentration-absorbance relationship curve shown in Figure 7B. This curve was constructed using the five-point method, achieving an R^2 value of ≥ 99%, which indicates a highly accurate correlation between concentration and absorbance. Using this relationship, the theoretical concentration of copper ions calculated for any given absorbance closely matches the actual concentration.

Through the relationship curve of concentration-absorbance obtained by UV-vis detection and analysis, we analysed the filtrate by UV-vis detection and analysis, and the detection method was the same as that of the standard sample. The efficiency of filtration was calculated by analysing the detection results after filtration and calculating the concentration of copper ions after filtration through the relationship curve in Fig.7B. The efficiency of filtration was calculated to be 87.3%, and the results are shown in Figure 7C. In addition, we also carried out repeated filtration experiments of

 doi:10.20944/preprints202404.1548.v1

Cu^{2+}, and the detection method of ion concentration after filtration was the same as that of the standard samples, and the results obtained from Figure 7B were used in the calculation of the filtrate concentration. In the cyclic filtration, the concentration of Cu^{2+} in each filtration was 8 mg/L, and the volume was 50 ml. After six times of cyclic filtration, the results obtained are shown in Figure 7D, The efficiency of filtration was basically unchanged in the first four filtrations, and the adsorption effect had a significant decrease from the fifth time onward, The decreasing factors of the adsorption results could be one of them is that the adsorption capacity of the nanofiber membrane might reach the limit, and the other one could be that the structure of the nanofiber membrane was damaged, which led to the decreasing of the adsorption effect.

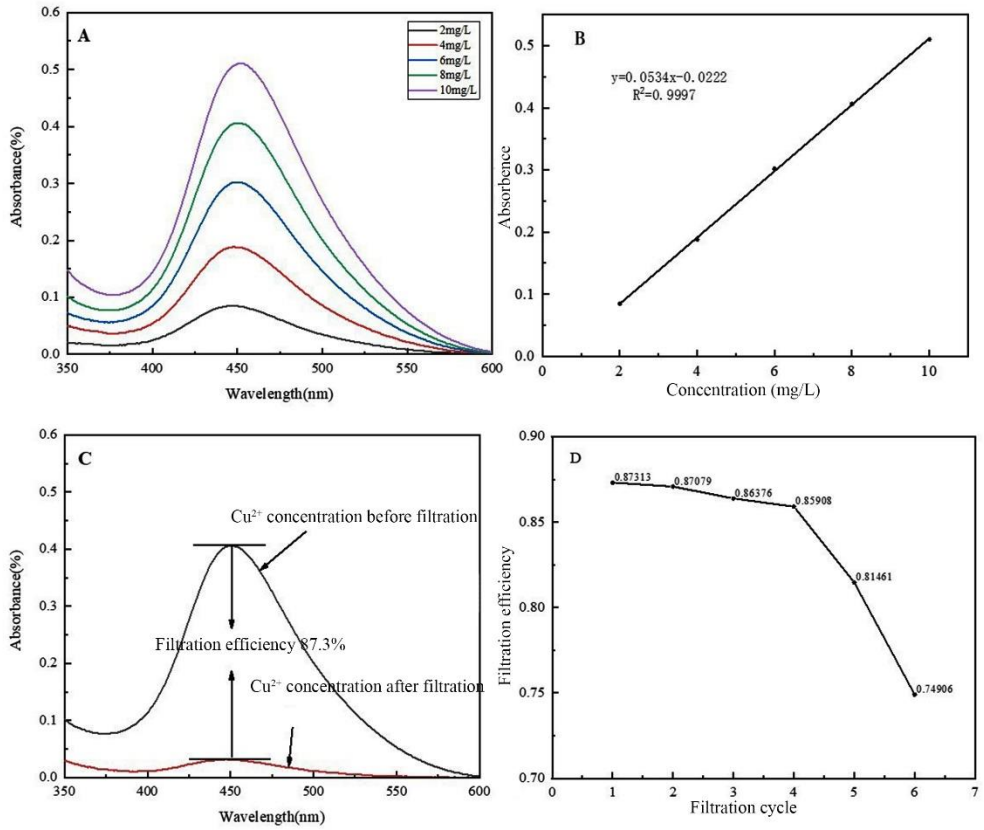

Figure 7. UV-vis detection results. (A) standard concentration Cu^{2+} detection results; (B) Cu^{2+} concentration versus absorbance; (C) Cu^{2+} filtration efficiency; (D) Cu^{2+} cyclic filtration efficiency.

4. Conclusions

In this study, SA/PEI/PVA multilayer composite nanofibrous membranes were prepared by electrostatic spinning technology, and a series of multilayer composite nanofibrous membranes were prepared by adjusting the parameters of the spinning process, and their structures and properties were fundamentally characterized using analytical test methods such as SEM, FTIR, EDS, UV-vis, XRD, TG, and so on. The results showed that the spinning process of the polymer solution could effectively change the microstructure of the nanofibers by reducing the injection speed and increasing the voltage, so that the spun nanofiber membranes were more uniform and continuous. The prepared SA/PEI/PVA multilayer composite nanofiber membrane can reach more than 85% adsorption efficiency of Cu(II) for a single time, and its adsorption efficiency of Cu(II) can still be maintained at more than 80% when it is reused for four times. The effective functional groups carboxyl (-COOH) and imino (-NH2) for Cu(II) adsorption on the prepared SA/PEI/PVA multilayer composite nanofiber membranes were analyzed by FTIR results.

Acknowledgments: This work was supported by the National Natural Science Foundation of China (51808263).

 doi:10.20944/preprints202404.1548.v1

References

1. Z. Wang, P. Luo, X. Zha, C. Xu, S. Kang, M. Zhou, D. Nover, Y. Wang, Overview assessment of risk evaluation and treatment technologies for heavy metal pollution of water and soil, Journal of Cleaner Production 379 (2022) 134043.
2. J.-y. Peng, S. Zhang, Y. Han, B. Bate, H. Ke, Y. Chen, Soil heavy metal pollution of industrial legacies in China and health risk assessment, Science of the Total Environment 816 (2022) 151632.
3. S. Wu, W. Shi, K. Li, J. Cai, L. Chen, Recent advances on sustainable bio-based materials for water treatment: Fabrication, modification and application, Journal of Environmental Chemical Engineering 10(6) (2022) 108921.
4. Z. Li, L. Yin, S. Jiang, L. Chen, S. Sang, H. Zhang, A photocatalytic degradation self-cleaning composite membrane for oil-water separation inspired by light-trapping effect of moth-eye, Journal of Membrane Science 669 (2023) 121337.
5. W. Shi, C. Xu, J. Cai, S. Wu, Advancements in material selection and application research for mixed matrix membranes in water treatment, Journal of Environmental Chemical Engineering (2023) 111292.
6. S. Wu, W. Shi, L. Cui, C. Xu, Enhancing contaminant rejection efficiency with ZIF-8 molecular sieving in sustainable mixed matrix membranes, Chemical Engineering Journal 482 (2024) 148954.
7. Y. Li, J. Zhu, H. Cheng, G. Li, H. Cho, M. Jiang, Q. Gao, X. Zhang, Developments of advanced electrospinning techniques: A critical review, Advanced Materials Technologies 6(11) (2021) 2100410.
8. M. Rahmati, D.K. Mills, A.M. Urbanska, M.R. Saeb, J.R. Venugopal, S. Ramakrishna, M. Mozafari, Electrospinning for tissue engineering applications, Progress in Materials Science 117 (2021) 100721.
9. A. Luraghi, F. Peri, L. Moroni, Electrospinning for drug delivery applications: A review, Journal of Controlled release 334 (2021) 463-484.
10. S. Wu, W. Shi, K. Li, J. Cai, C. Xu, L. Gao, J. Lu, F. Ding, Chitosan-based hollow nanofiber membranes with polyvinylpyrrolidone and polyvinyl alcohol for efficient removal and filtration of organic dyes and heavy metals, International Journal of Biological Macromolecules 239 (2023) 124264.
11. X. Li, W. Chen, Q. Qian, H. Huang, Y. Chen, Z. Wang, Q. Chen, J. Yang, J. Li, Y.W. Mai, Electrospinning-based strategies for battery materials, Advanced Energy Materials 11(2) (2021) 2000845.
12. D. Yang, L. Li, B. Chen, S. Shi, J. Nie, G. Ma, Functionalized chitosan electrospun nanofiber membranes for heavy-metal removal, Polymer 163 (2019) 74-85.
13. W. Shi, J. Cai, Y. Yang, C. Xu, J. Lu, S. Wu, Electrospun Carboxymethyl Cellulose/Polyvinyl Alcohol Nanofiber Membranes for Enhanced Metal Ion Removal, Sustainability 15(14) (2023) 11331.
14. O.D. Frent, L.G. Vicas, N. Duteanu, C.M. Morgovan, T. Jurca, A. Pallag, M.E. Muresan, S.M. Filip, R.-L. Lucaciu, E. Marian, Sodium alginate—natural microencapsulation material of polymeric microparticles, International Journal of Molecular Sciences 23(20) (2022) 12108.
15. M.A.J. Shaikh, G. Gupta, O. Afzal, M.M. Gupta, A. Goyal, A.S.A. Altamimi, S.I. Alzarea, W.H. Almalki, I. Kazmi, P. Negi, Sodium alginate-based drug delivery for diabetes management: A review, International journal of biological macromolecules 236 (2023) 123986.
16. Q. Wei, J. Zhou, Y. An, M. Li, J. Zhang, S. Yang, Modification, 3D printing process and application of sodium alginate based hydrogels in soft tissue engineering: A review, International Journal of Biological Macromolecules 232 (2023) 123450.
17. Q. Wang, L. Li, Y. Tian, L. Kong, G. Cai, H. Zhang, J. Zhang, W. Zuo, B. Wen, Shapeable amino-functionalized sodium alginate aerogel for high-performance adsorption of Cr (VI) and Cd (II): Experimental and theoretical investigations, Chemical Engineering Journal 446 (2022) 137430.
18. Y. Yang, X. Yu, Y. Zhu, Y. Zeng, C. Fang, Y. Liu, S. Hu, Y. Ge, W. Jiang, Preparation and application of a colorimetric film based on sodium alginate/sodium carboxymethyl cellulose incorporated with rose anthocyanins, Food Chemistry 393 (2022) 133342.
19. A. Verma, S. Thakur, G. Mamba, R.K. Gupta, P. Thakur, V.K. Thakur, Graphite modified sodium alginate hydrogel composite for efficient removal of malachite green dye, International journal of biological macromolecules 148 (2020) 1130-1139.
20. E.G. Arafa, M.W. Sabaa, R.R. Mohamed, E.M. Kamel, A.M. Elzanaty, A.M. Mahmoud, O.F. Abdel-Gawad, Eco-friendly and biodegradable sodium alginate/quaternized chitosan hydrogel for controlled release of urea and its antimicrobial activity, Carbohydrate Polymers 291 (2022) 119555.

 doi:10.20944/preprints202404.1548.v1

21. T. Li, H. Wei, Y. Zhang, T. Wan, D. Cui, S. Zhao, T. Zhang, Y. Ji, H. Algadi, Z. Guo, Sodium alginate reinforced polyacrylamide/xanthan gum double network ionic hydrogels for stress sensing and self-powered wearable device applications, Carbohydrate Polymers 309 (2023) 120678.
22. D.D. Al-Araji, F.H. Al-Ani, Q.F. Alsalhy, Polyethyleneimine (PEI) grafted silica nanoparticles for polyethersulfone membranes modification and their outlooks for wastewater treatment-a review, International Journal of Environmental Analytical Chemistry 103(16) (2023) 4752-4776.
23. S. Dube, R. Moutloali, S. Malinga, Hyperbranched polyethyleneimine/multi-walled carbon nanotubes polyethersulfone membrane incorporated with Fe-Cu bimetallic nanoparticles for water treatment, Journal of Environmental Chemical Engineering 8(4) (2020) 103962.
24. A.A. Shati, M.Y. Alfaifi, S.E.I. Elbehairi, B.D. Olegovich, R.H. Althomali, S.S. Abdullaev, E.A.M. Saleh, B.M. Hussien, M.K. Abid, M. Alwave, Functionalization of porous silica with graphene oxide and polyethyleneimine, containing zinc copper ferrite nanoparticles for water treatment and antibacterial application, Environmental Pollution (2024) 123745.
25. J. Xiang, H. Li, Y. Hei, G. Tian, L. Zhang, P. Cheng, J. Zhang, N. Tang, Preparation of highly permeable electropositive nanofiltration membranes using quaternized polyethyleneimine for dye wastewater treatment, Journal of Water Process Engineering 48 (2022) 102831.
26. S. Xiong, C. Han, A. Phommachanh, W. Li, S. Xu, Y. Wang, High-performance loose nanofiltration membrane prepared with assembly of covalently cross-linked polyethyleneimine-based polyelectrolytes for textile wastewater treatment, Separation and Purification Technology 274 (2021) 119105.
27. W. Gao, M.R. Razanajatovo, Y. Song, X. Zhao, Z. Zhao, Q. Peng, T. Jiao, X. Liu, Q. Zhang, Efficient heavy metal sequestration from water by Mussel-inspired polystyrene conjugated with polyethyleneimine (PEI), Chemical Engineering Journal 429 (2022) 132599.
28. F. Bucatariu, C.-A. Ghiorghita, M.-M. Zaharia, S. Schwarz, F. Simon, M. Mihai, Removal and separation of heavy metal ions from multicomponent simulated waters using silica/polyethyleneimine composite microparticles, ACS applied materials & interfaces 12(33) (2020) 37585-37596.
29. M.A. Tofighy, T. Mohammadi, Divalent heavy metal ions removal from contaminated water using positively charged membrane prepared from a new carbon nanomaterial and HPEI, Chemical Engineering Journal 388 (2020) 124192.